

# Preparation and Characterization of Bipolar Membranes Modified Using Photocatalyst Nano-TiO<sub>2</sub> and Nano-ZnO

Riyao Chen,<sup>1</sup> Yanyu Hu,<sup>1</sup> Zhen Chen,<sup>1,2</sup> Xiao Chen,<sup>1</sup> Xi Zheng<sup>1</sup>

<sup>1</sup>College of Chemistry and Materials Science, Fujian Normal University, Fuzhou 350007, People's Republic of China

<sup>2</sup>Chemistry Department of Fujian Ningde Teachers College, Ningde 352100, People's Republic of China

Received 6 November 2010; accepted 28 January 2011

DOI 10.1002/app.34247

Published online 21 May 2011 in Wiley Online Library (wileyonlinelibrary.com).

**ABSTRACT:** The nano-ZnO and nano-TiO<sub>2</sub> were added into chitosan (CS) anion layer to prepare polyvinyl alcohol (PVA) - sodium alginate (SA)/ TiO<sub>2</sub>-ZnO-CS (here, PVA:polyvinyl alcohol; SA:sodium alginate) bipolar membrane (BPM), which was characterized using scanning electron microscopy, atomic force microscopy (AFM), thermogravimetric analysis (TG), electric universal testing machine, contact angle measurer, and so on. Experimental results showed that nano-TiO<sub>2</sub>-ZnO exhibited better photocatalytic property for water splitting at the interlayer of BPM than nano-TiO<sub>2</sub> or nano-ZnO. The membrane impedance and voltage drop (IR drop) of the BPM were obviously

decreased under the irradiation of high-pressure mercury lamps. At a current density of 60 mA/cm<sup>2</sup>, the cell voltage of PVA-SA/TiO<sub>2</sub>-ZnO-CS BPM-equipped cell decreased by 1.0 V. And the cell voltages of PVA-SA/TiO<sub>2</sub>-CS BPM-equipped cell and PVA-SA/ZnO-CS BPM-equipped cell were only reduced by 0.7 and 0.6 V, respectively. Furthermore, the hydrophilicity, thermal stability, and mechanical properties of the modified BPM were increased. © 2011 Wiley Periodicals, Inc. *J Appl Polym Sci* 122: 1245–1250, 2011

**Key words:** bipolar membrane; photocatalysis; water splitting; nano-ZnO; nano-TiO<sub>2</sub>

## INTRODUCTION

Bipolar membranes (BPMs) comprise an important area of membrane research. Usually, a BPM is composed of a cation exchange layer, an anion exchange layer, and an interlayer, which consists of the area between the cation layer and the anion layer.<sup>1,2</sup> With the help of an electrical field, protons and hydroxide ions are generated by water splitting at the interlayer and migrate into the cathode chamber and the anode chamber, respectively.<sup>3–5</sup>

BPMs have been applied in industries for pollutant control, resource recovery, and chemical processing with a simple process, high efficiency, and low waste disposal.<sup>6–9</sup>

The BPM potential depends largely on the IR drop of the interlayer.<sup>10</sup> The BPMs with excellent performances such as high water-splitting efficiency and low membrane impedance are expected. Recently, more and more attention has been paid to modification of cation layer or anion layer, and introduction of catalytic interlayer to promote water splitting.<sup>11</sup>

Simons found that water splitting of a BPM was promoted when the cation or anion layer was coated with one or more suitable inorganic electrolyte such as sodium metasilicate, chromic nitrate, ruthenium trichloride, or indium sulfate.<sup>12</sup>

Xu et al. prepared the anion layers with different ammonium groups by reacting the bromomethylated poly(2,6-dimethyl-1,4-phenylene oxide) (BPPO) with different amines, and then the corresponding BPMs were prepared by casting the sulfonated poly(phenylene oxide) (PPO) solution on these anion exchange layers. They found that water splitting was too much extent related with pK<sub>b</sub> value of amines.<sup>13</sup>

Wakamatsu et al. prepared cation-exchange fiber (CEF) and anion-exchange fiber (AEF) fabrics as the interlayer of a BPM by electrospray deposition and postdeposition chemical modification. Experimental results showed that the AEF fabrics enhanced water splitting, and the CEF fabrics reduced water splitting.<sup>14</sup>

Chen et al.<sup>15</sup> reported that SA/CS BPM was modified by copper phthalocyanine tetrasulfonic acid and copper tetra-aminophthalocyanine, respectively, which could reduce the membrane impedance and IR drop of the BPM.

TiO<sub>2</sub>, as a photocatalyst, is possessed of many advantages such as high photocatalytic activity, good chemical stability, resistance to light corrosion, harmless to human body, and so on.<sup>16</sup> Previous studies indicated that the photocatalytic activity of

Correspondence to: R. Chen (rychen@fjnu.edu.cn).

Contract grant sponsor: Natural Science Foundation of the Fujian Province of China; contract grant number: D0710009.

ZnO-doped TiO<sub>2</sub> would be enhanced.<sup>17</sup> In addition, when inorganic nanoparticles were added into polymer material, the mechanical properties and thermal stability would be improved due to the surface effect and interfacial action of the nanoparticles.<sup>18</sup>

In this article, nano-ZnO and nano-TiO<sub>2</sub> were added into PVA-SA/CS BPM to promote water splitting, reduce membrane impedance, and improve the thermal stability and mechanical properties of the BPM. The decrease of membrane impedance and cell voltage would help to inhibit the side electrochemical reactions in the chambers.

## EXPERIMENTAL

### Materials

Sodium alginate, chitosan (CS) with an N-deacetylation degree of 90%, nano-ZnO, nano-TiO<sub>2</sub>, and glutaraldehyde (25% by volume in water) were purchased from Guoyao Chemicals. Other chemicals were analytical grade.

### Preparation of BPMs

#### Preparation of PVA-SA/TiO<sub>2</sub>-ZnO-CS BPM

PVA aqueous solution (100 mL 6.0 wt %) was added into 100 mL of 3.0-wt % SA aqueous solution, and then the PVA-SA solution was poured onto a glass plate and dried at room temperature. The membrane was cross-linked with FeCl<sub>3</sub> solution (9.0 wt %) for 30 min and dried to form PVA-SA cation exchange membrane (area 50 cm<sup>2</sup>).

The TiO<sub>2</sub>-ZnO-CS solution was made by mixing 100 mL 3.0-wt % CS aqueous solution, 80-mL nano-ZnO (0.01 g), and nano-TiO<sub>2</sub> (0.01 g) alcohol solution, and 3-mL glutaraldehyde (0.25% by volume in water) and stirring for 30 min. The TiO<sub>2</sub>-ZnO-CS solution was poured over the prepared PVA-SA membrane and dried to form the PVA-SA/TiO<sub>2</sub>-ZnO-CS BPM.

#### Preparation of PVA-SA/TiO<sub>2</sub>-CS BPM

In comparison with PVA-SA/TiO<sub>2</sub>-ZnO-CS BPM, the PVA-SA/TiO<sub>2</sub>-CS BPM was prepared. The preparation method of PVA-SA/TiO<sub>2</sub>-CS BPM was similar to that of PVA-SA/TiO<sub>2</sub>-ZnO-CS BPM, except that nano-ZnO was not added into the CS aqueous solution in the preparing process of the CS anion membrane.

#### Preparation of PVA-SA/ZnO-CS BPM

In comparison with PVA-SA/TiO<sub>2</sub>-ZnO-CS BPM, the PVA-SA/ZnO-CS BPM was prepared. The preparation method of PVA-SA/ZnO-CS BPM was similar to that of PVA-SA/TiO<sub>2</sub>-ZnO-CS BPM, except that

nano-TiO<sub>2</sub> was not added into the CS aqueous solution in the preparing process of the CS anion membrane.

### Characterization of BPMs

#### Scanning electron microscopy analysis of BPM

The morphology of the interlayer of PVA-SA/TiO<sub>2</sub>-ZnO-CS BPM was observed by a scanning electron microscopy (SEM; XT30 ESEM-TMP, Philips).

#### Atomic force microscopy observation of TiO<sub>2</sub>-ZnO-CS membrane

Nanoscope Multimode IIIa scanning probe microscopy (Veeco Instruments) was used to observe the surface morphology of the TiO<sub>2</sub>-ZnO-CS membrane.

#### Measurement of the thermal stability of BPM

The thermal stability of the BPM was evaluated with thermogravimetric analysis (TG) analyzer (NETZSCH STA 449C). The investigation temperature was from room temperature to 600°C at a heating rate of 10°C/min. All the samples were performed under dynamic nitrogen.

#### Determination of mechanical properties of BPM

The mechanical properties of the BPMs were measured using electric universal testing machine (CMT6104, Shenzhen Sans Testing Machine in China). And the tensile strength is calculated as follows:

$$\delta_t = P/bd \quad (1)$$

Here,  $\delta_t$  is the tensile strength (MPa);  $b$  is the width of BPM sample (mm);  $d$  is the thickness of BPM sample (mm);  $P$  is the maximum load (N).

#### Determination of hydrophilicity of CS membrane

The contact angles of CS membranes before and after modification with nano-ZnO, nano-TiO<sub>2</sub>, or nano-TiO<sub>2</sub>-ZnO were determined using contact angle measurer [SL 200B, S & L (Shanghai) in China]. The smaller the contact angle is, the stronger the hydrophilicity of a membrane will be.

#### Measurement of current–voltage curve of BPM-equipped cell

The current–voltage ( $J$ – $V$ ) curve of the modified BPM-equipped cell was measured using a direct current source (DF1720SB5A, Ningbo Zhongce Electronics in China). The experimental equipment was shown in Figure 1.

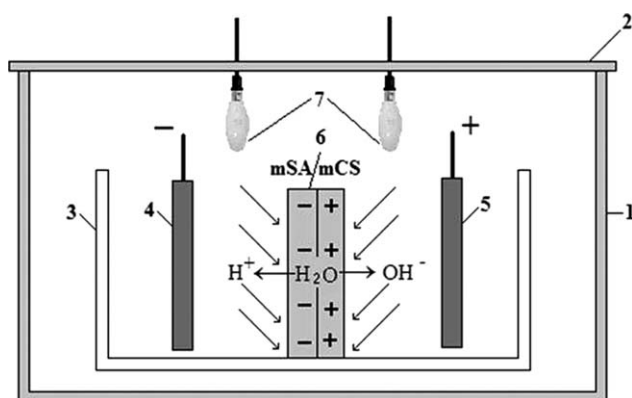


**Figure 1** Schematic diagram of the experimental equipment: 1, box shell; 2, lid; 3, electrolysis cell; 4, cathode; 5, anode; 6, BPM; 7, high-pressure mercury lamps.

The BPM was fixed between the cathode chamber and the anode chamber as a separator. The catholyte and the anolyte were both 250 mL 1.0 mol/L  $\text{Na}_2\text{SO}_4$  solution. The anode and cathode were both Pb electrodes (area  $2 \text{ cm}^2$ ). After the lid was put on, the  $J$ - $V$  curve was measured. Next, the high-pressure mercury lamps were turned on, and the  $J$ - $V$  curve was measured once more.

Under the same conditions, the  $J$ - $V$  curve was measured without membrane between the two half-cells. The difference between the cell voltages of BPM-equipped cell and undivided cell was the IR drop of the BPM.<sup>15</sup>

## RESULTS AND DISCUSSION

### SEM of PVA-SA/TiO<sub>2</sub>-ZnO-CS BPM

The scanning electron micrograph of PVA-SA/TiO<sub>2</sub>-ZnO-CS BPM was presented in Figure 2. Two dis-

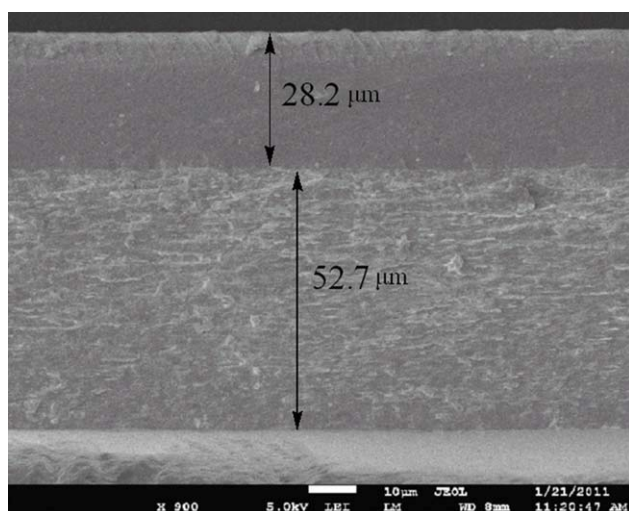


**Figure 2** SEM of PVA-SA/TiO<sub>2</sub>-ZnO-CS BPM. [Color figure can be viewed in the online issue, which is available at [wileyonlinelibrary.com](http://wileyonlinelibrary.com).]

tinct layers in the BPM were observed. The bottom layer was the TiO<sub>2</sub>-ZnO-CS anion exchange layer (approximately  $52.7 \mu\text{m}$  thick), while the upper layer was the PVA-SA cation exchange layer (approximately  $28.2 \mu\text{m}$  thick). The two layers were closely combined with each other, and there was no bubble or crack at the interlayer with a thickness in nanometer range.

### AFM of TiO<sub>2</sub>-ZnO-CS membrane

The atomic force microscopy (AFM) image of TiO<sub>2</sub>-ZnO-CS membrane was shown in Figure 3. The nanoparticles were uniformly distributed on the surface of the TiO<sub>2</sub>-ZnO-CS membrane. The sizes of nanoparticles were smaller than 100 nm. The surface of the membrane was smooth and compact, and no pinhole was observed.

### Mechanical properties of PVA-SA/TiO<sub>2</sub>-ZnO-CS BPM

The mechanical properties of the different BPMs were listed in Table I. The elongation rate rose when the nano-TiO<sub>2</sub>-ZnO was added into PVA-SA/CS BPM. Introduction of nanoparticles into CS anion layer destroyed the intermolecular hydrogen bonds of CS chains, which formed between  $-\text{OH}$  and  $-\text{NH}_2$ , lowered the crystallinity of membrane and increased the flexibility of CS chains. According to the crack pinning theory, nanoparticles may act as

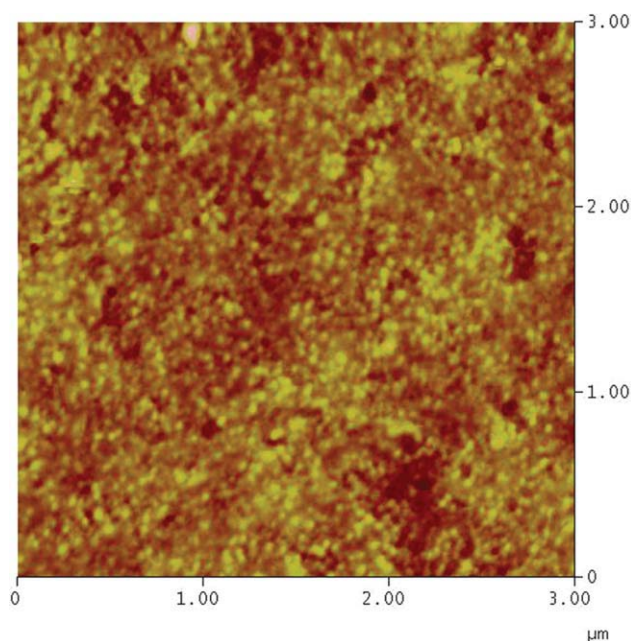


**Figure 3** AFM image of TiO<sub>2</sub>-ZnO-CS membrane. [Color figure can be viewed in the online issue, which is available at [wileyonlinelibrary.com](http://wileyonlinelibrary.com).]



**TABLE I**  
**Mechanical Properties of the Different BPMs**

BPM	Maximum load (N)	Tensile strength (MPa)	Elongation rate (%)	Young's modulus (MPa)
PVA-SA/CS	37.741	12.580	81.29	30.68
PVA-SA/ZnO-CS	48.442	21.062	63.85	50.07
PVA-SA/TiO <sub>2</sub> -CS	52.859	26.430	93.96	63.86
PVA-SA/TiO <sub>2</sub> -ZnO-CS	57.496	28.748	94.68	82.48

obstacles to crack growth by pinning, which also improved the elongation rate of the membrane.<sup>19</sup>

In addition, the tensile strength, maximum load, and Young's modulus were noticeably increased, and the mechanical properties were enhanced evidently. The characteristics of nanoparticles such as higher rigidity than polymer molecular, high specific surface area, and sufficient particle-matrix adhesion should be credited for the improvement of mechanical properties. A large number of  $-OH$  groups existed on the surface of nanoparticles.  $-NH_2$  groups in CS chains were protonated to form  $-NH_3^+$ , which could subsequently connect with  $-OH$  groups of nanoparticles through hydrogen bonds to form net structure. Also, nanoparticles had strong attractive force due to large specific surface area. The CS chains could be attracted to the surface of nanoparticles, which acted as crosslinking points in the membrane. Besides the above two factors, stresses transfer and elastic deformation from matrix to nanoparticles could also improve the mechanical properties of membrane.

#### Thermal stability of PVA-SA/TiO<sub>2</sub>-ZnO-CS BPM

The TG curves of PVA-SA/CS BPM and PVA-SA/TiO<sub>2</sub>-ZnO-CS BPM were shown in Figure 4. Both of the BPMs were decomposed in steps, which corresponded to the loss of physical adsorption water and the decomposition of macromolecular chains, respectively. After modification, the TG curve shifted to high temperature zone, which indicated that the thermal stability of the modified BPM was improved. According to the above discussion, CS chains were combined with nanoparticles through hydrogen bonds and the attraction of nanoparticles to form net structure in the membrane, which helped to improve the interaction force between CS chains and nanoparticles, and blocked the movement of CS chains during heating. It meant that the decomposition of CS chains would need more energy, resulting in the increase of thermal stability.

#### Hydrophilicity of the modified CS membrane

The contact angles of CS membranes modified by nano-ZnO, nano-TiO<sub>2</sub>, or nano-TiO<sub>2</sub>-ZnO were

shown in Figure 5. After modification, the contact angle of CS membrane decreased from 104.01° [Fig. 5(a)] to 84.62° [Fig. 5(b)], 34.65° [Fig. 5(c)], and 24.99° [Fig. 5(d)], respectively. Because a large number of  $-OH$  groups existed on the surface of nanoparticles, the hydrogen bonds formed between water molecules and nanoparticles, which led to the improvement in hydrophilicity of the modified CS membrane.

#### J-V curve of BPM-equipped cell

The J-V curves of the modified BPM-equipped cell before and after UV irradiation were shown in Figure 6 (curves C and E were the J-V curves of PVA-SA/CS BPM-equipped cell and the undivided cell, respectively). At a current density of 60 mA/cm<sup>2</sup>, the cell voltages of PVA-SA/TiO<sub>2</sub>-CS BPM-equipped cell (curves B and b) and PVA-SA/ZnO-CS BPM-equipped cell (curves A and a) decreased by 0.7 and 0.6 V, respectively, under the irradiation of high-pressure mercury lamps because of the photocatalytic function and high photon efficiency of nano-ZnO and nano-TiO<sub>2</sub>.

The cell voltage of PVA-SA/TiO<sub>2</sub>-ZnO-CS BPM-equipped cell (curves D and d) decreased by 1.0 V under the irradiation of high-pressure mercury lamps. As shown in Figure 7, because the

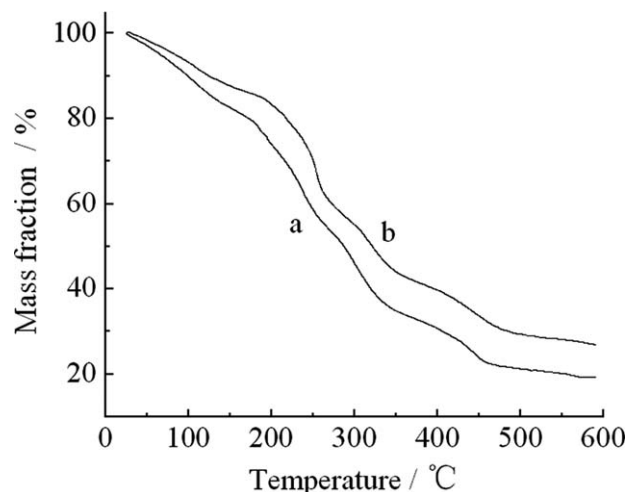


**Figure 4** TG curves of the BPMs. (a) PVA-SA/CS BPM and (b) PVA-SA/TiO<sub>2</sub>-ZnO-CS BPM.

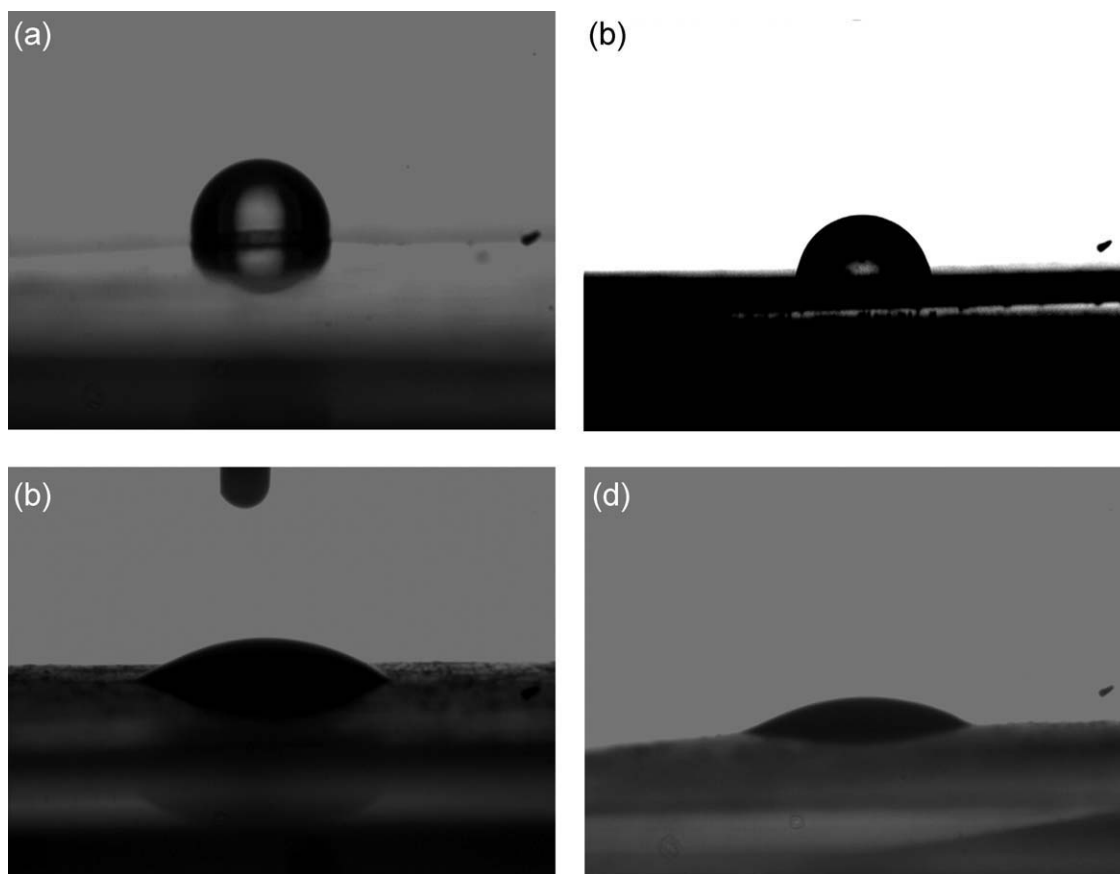


**Figure 5** The contact angles of the CS membranes (a) CS membrane; (b) ZnO-CS membrane; (c) TiO<sub>2</sub>-CS membrane; (d) TiO<sub>2</sub>-ZnO-CS membrane.

conduction band of ZnO is higher than that of ZnO, the photoexcited electron on the conduction band of ZnO is rapidly transferred to the conduction band of

TiO<sub>2</sub>, which leads to a high efficiency for the separation of photoexcited electron and photoexcited hole. Therefore, the recombination rate of photoexcited carriers is reduced, and the photocatalytic efficiency for water splitting is improved.

In addition, modification using nano-TiO<sub>2</sub>-ZnO could dramatically reduce the cell voltage of PVA-SA/CS BPM-equipped cell (curves C and D) without UV irradiation. It was because the improvement in hydrophilicity of the modified CS membrane and interaction between membrane and water molecules

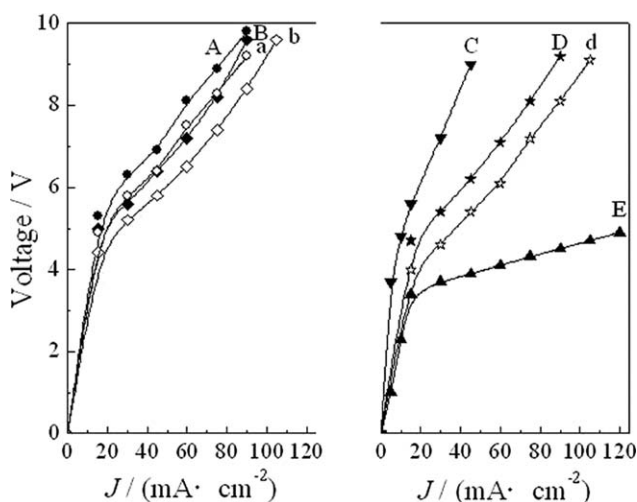


**Figure 6** *J*-*V* curves of the modified BPMs before and after UV irradiation: (A) PVA-SA/ZnO-CS BPM (no irradiation); (a) PVA-SA/ZnO-CS BPM (irradiation); (B) PVA-SA/TiO<sub>2</sub>-CS BPM (no irradiation); (b) PVA-SA/TiO<sub>2</sub>-CS BPM (irradiation); (C) PVA-SA/CS BPM; (D) PVA-SA/TiO<sub>2</sub>-ZnO-CS BPM (no irradiation); (d) PVA-SA/TiO<sub>2</sub>-ZnO-CS BPM (irradiation); (E) no membrane.

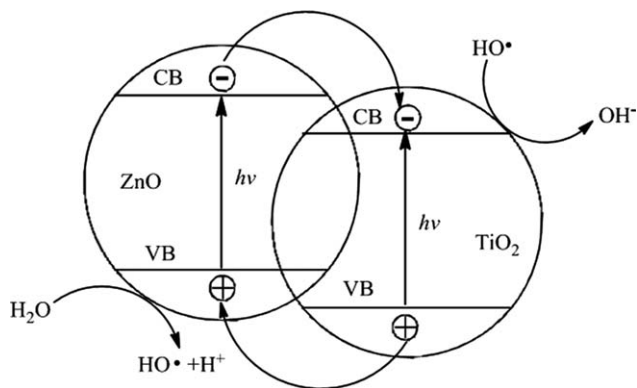


**Figure 7** Mechanism of photocatalytic water splitting.

relaxed the molecule bonds in water, promoted water molecules easily splitting to protons and hydroxide ions, and decreased membrane impedance and IR drop.

### CONCLUSIONS

The nano-ZnO and nano-TiO<sub>2</sub> were added into CS anion layer to prepare the PVA-SA/TiO<sub>2</sub>-ZnO-CS BPM, which was characterized using SEM, AFM, TG, electric universal testing machine, contact angle measurer, and so on.

Experimental results showed that nano-TiO<sub>2</sub>-ZnO coupled semiconductor appeared better photocatalytic property for water splitting at the interlayer of BPM than nano-TiO<sub>2</sub> or nano-ZnO. Under the irradiation of high-pressure mercury lamps, the membrane impedance and IR drop of the modified BPMs were evidently decreased.

Furthermore, the hydrophilicity, thermal stability, and mechanical properties of the modified BPM were increased. The increase in hydrophilicity of the BPM and the weakening of the bonding force of water molecule promoted water splitting at the interlayer, which reduced the membrane impedance and IR drop.

The authors thank Danmei Pan and Fujian Institute of Research on the Structure of Mater, Chinese Academy of Sciences for kind help in the AFM measurement.

### References

1. Hwang, U. S.; Choi, J. H. *Sep Purif Technol* 2006, 48, 16.
2. Bauer, B.; Gerner, F. J.; Strathmann, H. *Desalination* 1988, 68, 279.
3. Hsueh, C. H.; Peng, Y. J.; Wang, C. C. *J Membr Sci* 2003, 219, 1.
4. Wilhelm, F. G.; Van der Vegt, N. F. A.; Strathmann, H.; Westling, M. *J Appl Electrochem* 2002, 32, 455.
5. Atkinson, S. *Membr Technol* 2003, 149, 10.
6. Xu, T. W. *Resour Conservat Recycl* 2002, 37, 1.
7. Ren, Y. X.; Chen, Z.; Chen, R. Y.; Zheng, X.; Geng, Y. M. *Central Eur J Chem* 2007, 5, 177.
8. Schaffner, F.; Pontalier, P. Y.; Sanchez, V.; Lutin, F. *Desalination* 2004, 170, 113.
9. Mafe, S.; Ramirez, P.; Alcaraz, A.; Aguilera, V. M. *Handbook of Bipolar Membrane Technology*, Twente University Press: Enschede, 2000, 49.
10. Xu, T. W.; Wang, W. Z.; Liu, N. *Technol Water Treatment* 1998, 24, 20.
11. Hao, J. H.; Chen, C. X.; Li, L.; Yu, L. X.; Jiang, W. J. *J Appl Polym Sci* 2001, 80, 1658.
12. Simons, R. *Electrochim Acta* 1986, 31, 1175.
13. Xu, T. W.; Fu, R. Q.; Yang, W. H.; Xue, Y. H. *J Membr Sci* 2006, 279, 282.
14. Wakamatsu, Y.; Matsumoto, H.; Minagawa, M.; Tanioka, A. *J Colloid Interface Sci* 2006, 300, 442.
15. Chen, R. Y.; Chen, Z.; Zheng, X.; Chen, X.; Huang, C. X. *J Membr Sci* 2010, 355, 1.
16. Mor, G. K.; Shankar, K.; Paulose, M.; Varghese, O. K.; Grimes, C. A. *Nano Lett* 2006, 6, 215.
17. Lin, K.; Tsai, P. *Mater Sci Eng B* 2007, 139, 81.
18. Ji, X. L.; Jing, J. K.; Jiang, W.; Jiang, B. Z. *Polym Eng Sci* 2002, 42, 983.
19. Green, D. J.; Nicholson, P. S.; Embury, J. D. *J Mater Sci* 1979, 14, 1657.